Computational and Structural Biotechnology Journal 23 (2024) 2754–2762

Contents lists available at ScienceDirect

Computational and Structural Biotechnology Journal

journal homepage: www.elsevier.com/locate/csbj

Research article

A global view of altered ligand-receptor interactions in bone marrow aging based on single-cell sequencing

Wenbo Chen [a,1], Xin Chen [b,1], Lei Yao [b,1], Jing Feng [c], Fengyue Li [b], Yuxin Shan [b], Linli Ren [b], Chenjian Zhuo [b], Mingqian Feng [b], Shan Zhong [a,*], Chunjiang He [b,*]

[a] School of Basic Medical Sciences, Taikang Medical School, Wuhan University, Wuhan 430071, China
[b] College of Biomedicine and Health, Huazhong Agricultural University, Wuhan 430070, China
[c] School of Computer Science, Wuhan University, Wuhan 430072, China

ARTICLE INFO

Keywords:
Cell-cell interaction
Ligand and receptor
Single-cell transcriptome
Bone marrow
Aging

ABSTRACT

Altered cell-cell communication is a hallmark of aging, but its impact on bone marrow aging remains poorly understood. Based on a common and effective pipeline and single-cell transcriptome sequencing, we detected 384,124 interactions including 2575 ligand-receptor pairs and 16 non-adherent bone marrow cell types in old and young mouse and identified a total of 5560 significantly different interactions, which were then verified by flow cytometry and quantitative real-time PCR. These differential ligand-receptor interactions exhibited enrichment for the senescence-associated secretory phenotypes. Further validation demonstrated supplementing specific extracellular ligands could modify the senescent signs of hematopoietic stem cells derived from old mouse. Our work provides an effective procedure to detect the ligand-receptor interactions based on single-cell sequencing, which contributes to understand mechanisms and provides a potential strategy for intervention of bone marrow aging.

1. Introduction

Aging is a physiological process involving the decline of organ function, loss of homeostasis, and increased risk of disease [1]. Altered intercellular communication is one of the twelve major markers of aging [2]. For example, changes in FGF receptor 1 and p38αβ MAPK signaling pathways can cause senescence of resident muscle MSCs [3]. Some secreted factors mediate the senescence of neighboring cells by blocking growth factor signaling [4]. By blocking the activation of IκB kinase beta (IKK-β) and nuclear factor kappa B (NF-κB) in the aging hypothalamus or brain, aging can be delayed and lifespan extended [5]. Thus, deciphering the changes in intercellular communication associated with aging will help us understand the onset of aging and the diseases caused by aging. As an important hematopoietic organ, bone marrow is also significantly affected by aging [6,7]. Previous research has revealed the interaction of non-hematopoietic cells of the niche and hematopoietic stem cells (HSCs) by flow cytometry [8]. However, a global view of changes of intercellular communication related to bone marrow aging remains insufficient.

While proteomic technologies are preferable method for the direct measurement of protein abundances, proteomics at single-cell resolution is still not mature. In contrast, transcriptome are easier to measure and straightforward to analyse. Therefore, single-cell transcriptome sequencing is an alternative method for detecting cell-cell interactions [9]. In previous work, single-cell transcriptome sequencing reveals the aberrant communications between stromal cells and hematopoietic cells in leukemia [10,11]. There are also several tools have been developed to analyze cell-cell interactions based on single-cell data, such as SingleCellSignalR [12], icellnet [13], Giotto [14], CellPhoneDB [15] and Cellchat [16]. Combined with the known ligand-receptor (LR) database, potential LR interactions between different cells can be easily inspected [9]. Therefore, it is reasonable to use single-cell sequencing to investigate changes of cell interactions in bone marrow aging.

In this study, we performed single-cell sequencing for bone marrow samples from old and young mice and used a common and effective pipeline to systematically identify the differential ligand-receptor

Abbreviations: LR, ligand and receptor; SASP, senescence-associated secretory phenotype; HSC, hematopoietic stem cells; RT-qPCR, quantitative real-time PCR; ECM, Extracellular matrix; Igfbp4, insulin like growth factor binding protein 4; Mmp9, matrix metallopeptidase 9; Selenop, selenoprotein P.

* Corresponding authors.
E-mail addresses: zhongshan@whu.edu.cn (S. Zhong), che@whu.edu.cn (C. He).

[1] These authors contributed equally

https://doi.org/10.1016/j.csbj.2024.06.020
Received 25 March 2024; Received in revised form 17 June 2024; Accepted 18 June 2024
Available online 20 June 2024

interactions between old and young mice. The results reveal global alterations of ligand-receptor interactions in aging bone marrow, providing clues for the research of novel aging markers and potential intervention targets.

2. Results

2.1. Single-cell profiling of non-adherent bone marrow cells of old and young mice

Single-cell transcriptome sequencing was performed on bone marrow samples from 6 mice (3 old mice and 3 young mice). After quality control, a total of 32,172 and 42,827 high-quality cells from the old and young groups were retained for subsequent analysis (Fig. 1A). Using bone marrow cell makers collected from public databases and literature (See Methods), 16 cell types were finally annotated: B cell, Basophil, Erythroblast, Erythroid progenitor cell, Hematopoietic stem cell, Macrophage, Plasma cell, Monocyte, Naive B cell, Natural killer cell, Neutrophil, CD8 naive T cell, CD8 effector memory T cell, CD4 regulatory T cell, CD4 helper T cell 1 and CD4 follicular helper T cell. The proportion of cells with differentiation potential in the old group was significantly reduced, such as Hematopoietic stem cells, Erythroid progenitor cells, Naive B cells and CD8 naive T cells. In contrast, the proportion of terminally differentiated cells, such as Macrophage, Monocyte, CD8 effector memory T cells, CD4 regulatory T cells and B cells, increased significantly in the old group (Fig. 1B). This is consistent with previous reports [17,18].

2.2. Differences in ligand-receptor interactions between old and young mice

We used a common and effective pipeline to analyze differences in ligand-receptor (LR) interactions between multiple cells in old and young mice. We estimated the ligand and receptor interaction scores (LR scores) between each pair of ligand and receptor in different cells. The difference of LR scores between the two groups were then evaluated by a permutation test and a MS value was calculated (See Methods). We analyzed a total of 384,124 interactions including 2575 pairs of ligand and receptor expressed in 16 cell types (each cell may serve as a sender cell or a receiver cell). While the significance threshold (P value < 0.05) was met, a total of 13,186 interactions with $|MS| >= 0.05$ (including 10,000 pairs of $MS > 0.05$ and 3186 pairs of $MS < -0.05$) among all cell types were observed. Using a more stringent threshold, there are 5560 interactions with $|MS| >= 0.1$, including 4323 with $MS > 0.1$, which indicates higher interactions in old group and 1237 with $MS < -0.1$, which indicates higher interactions in young group (Table S1). These 5560 differential LR interactions involving 160 ligand genes, 144 receptor genes, and 256 cell pairs (16 ×16 cell types) were used for subsequent analysis (Fig. 2B).

We next examined which cell pairs had the most LR pairs that differed between old and young group. We found that among all cell interactions, Basophil - CD8 naive T cells involved the most differential LR pairs (52 pairs). Naive B cell - Erythroblast involves the least number of differential LR pairs (3 pairs). For sender cells, CD4 follicular helper T cells participate in the most differential LR interactions, with a total of 488 pairs of LRs. For receiver cells, CD8 naive T cells participated in the most differential LR interactions, with a total of 639 pairs of LRs (Fig. 2C).

Among all 5560 differential LR interactions, Thbs1|Cd47, Thbs1|Itga4, and Thbs1|Itgb1 were involved in the largest number of interactions, 221, 180, and 178, respectively (Fig. 2D). Previous work revealed Thbs1 (thrombospondin 1) is an adhesion glycoprotein that mediates cell-cell and cell-matrix interactions [19] and expressed during inflammation and exerts functions such as inhibiting angiogenesis and immune activity [20,21]. CD47 serves as both a ligand for signal regulatory protein α (SIRPα) and a receptor for Thbs1, mediating the phagocytosis of aging red blood cells [22]. The cell adhesion mediated by integrin family genes such as Igta4, Igtb1 and Itgb2 also plays an important role in cellular aging [23], which is also revealed by our analysis.

Among all differential LR interactions, Ccl5|Ccr5 between CD8 naive T cell and CD8 effector memory T cell, Ccl5|Ccr1 between CD8 naive T cell and Basophil, Hmgb1|Cxcr4 between Erythroid progenitor cell and CD4 follicular helper T cell, Hmgb1|Cxcr4 between Erythroid progenitor cell and CD4 regulatory T cell and Hmgb1|Cxcr4 between Erythroid progenitor cell and CD8 effector memory T cell has the largest MS value (>0.5), indicating that these LR interactions have the most significant increase in the old group. Ccl5 has been shown to be increased in the cortex of aging mice, which may be related to various aging processes [24]. Hmgb1 is involved in the function of muscle cells and participates in the appearance of aging phenotypes [25,26]. In contrast, Calm1|Sell between Natural killer cell and CD4 follicular helper T cell, Calm1|Sell between CD4 helper T cell 1 and CD4 follicular helper T cell, Calm1|Sell between B cell and CD4 follicular helper T cell, Calm1|Sell between

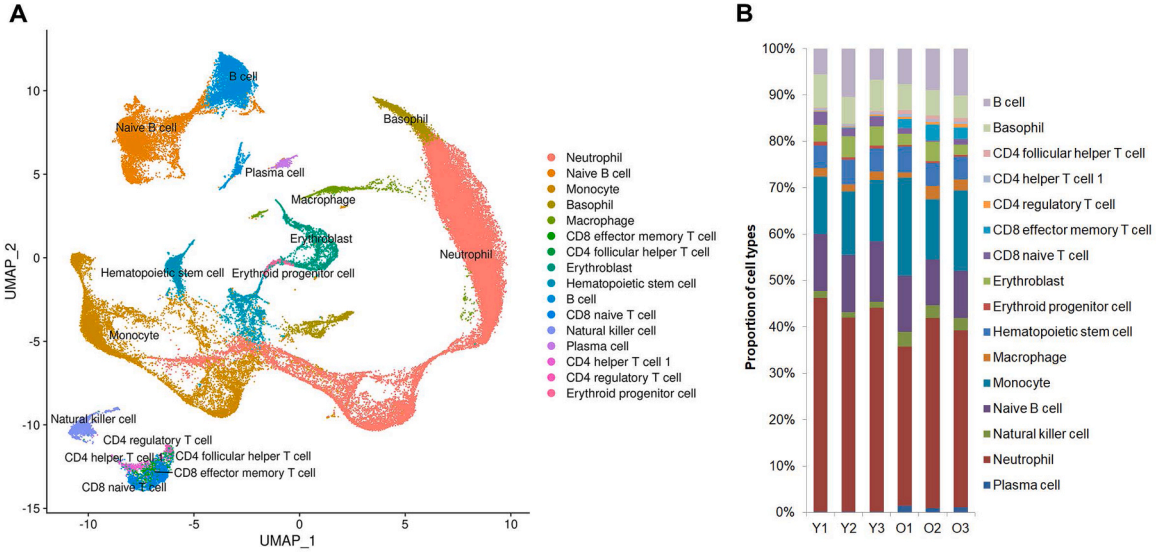

Fig. 1. Profiling of non-adherent bone marrow cells from old and young mice. A. Umap diagram shows clustering and annotation of old and young mouse non-adherent bone marrow cells. B. Histogram showing the proportion of non-adherent bone marrow cells in old and young mice.

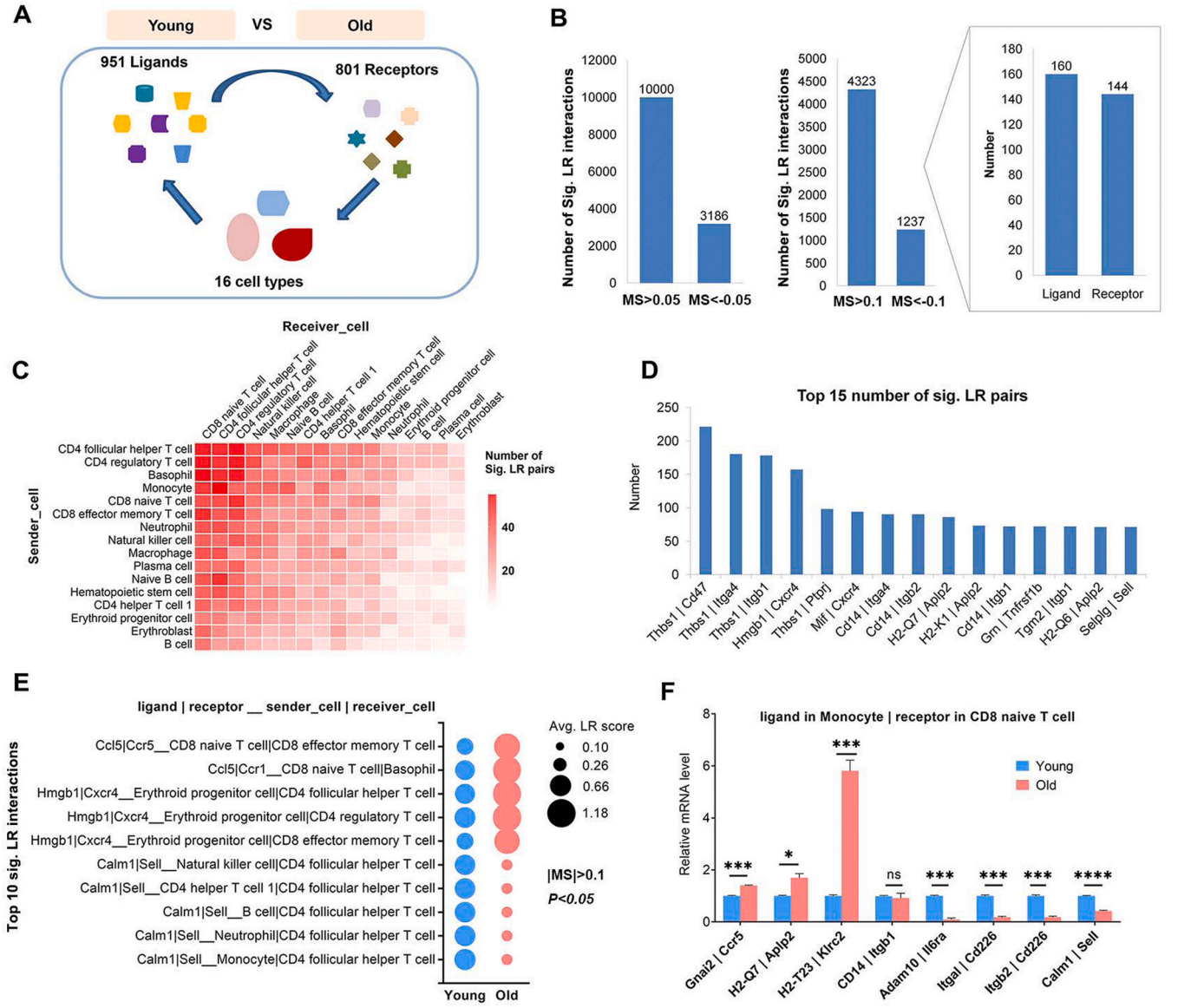

Fig. 2. Differential ligand-receptor interactions in old and young bone marrow. A. Schematic diagram of ligand-receptor interactions in old and young bone marrow. B. Left. The number of different LR interactions between old and young bone marrow when the threshold is |MS| >=0.05 and P < 0.05. Middle. The number of different LR interactions between old and young bone marrow when the threshold is |MS| >=0.1 and P < 0.05. Right. The number of ligands and receptors involved in differential LR interactions when the threshold is |MS| >=0.1 and P < 0.05. C. Distribution of differential LR pairs among 16 cell types. D. The top 15 pairs of LR that participate in the most differential LR interactions. E. The 10 most significant different LR interactions between the bone marrow of old and young mice. Five were up-regulated and five were down-regulated in old group. The size of the points represents the average LR score of each group of samples. F. RT-qPCR verification of 8 different LR pairs between Monocyte and CD8 naïve T cells. * P-value< 0.05, ** P-value< 0.01, *** P-value< 0.001.

Neutrophil and CD4 follicular helper T cell and Calm1|Sell between Monocyte and CD4 follicular helper T cell had the smallest MS values (<−0.4) (Fig. 2E), indicating that these LR interactions were most significantly reduced in the old group. As Calm1 (encoding CaM) tend to decrease in aging organs such as the brain [27] and Sell (L-selectin) decreases with the aging of polymorphonuclear neutrophils [28,29], our results also suggest the importance of these molecules in bone marrow aging.

To validate our calculations, we used differential LR interactions between Monocytes and CD8-naïve T cells. Bone marrow samples from old and young mice were obtained respectively, and their Monocytes and CD8 naïve T cells were sorted using corresponding flow cytometry antibodies (Fig. S1). We extracted the most significant 8 pairs of LR between Monocytes and CD8 naive T cells, 4 pairs were up-regulated and 4 pairs were down-regulated in aged mice. RT-qPCR confirmed the expression trend of 7 pairs of LR, except one pair had no significant difference between old and young bone marrow (Fig. 2F).

2.3. *Functional implications of differential ligand-receptor interactions in bone marrow aging*

As ligand-receptor interactions mainly affect downstream signaling pathways [30], we analyzed the downstream pathways of differential LR interactions in old and young mice. We performed KEGG pathway enrichment on 144 receptor genes involved in 5560 differential LR interactions and found that these receptors are mainly enriched in the cell adhesion molecules, hematopoietic cell lineage, cytokine-cytokine receptor interaction and ECM-receptor interaction pathways (Fig. 3A). These pathways have been reported to be closely related to aging. For example, cell adhesion molecules play an important role in brain aging

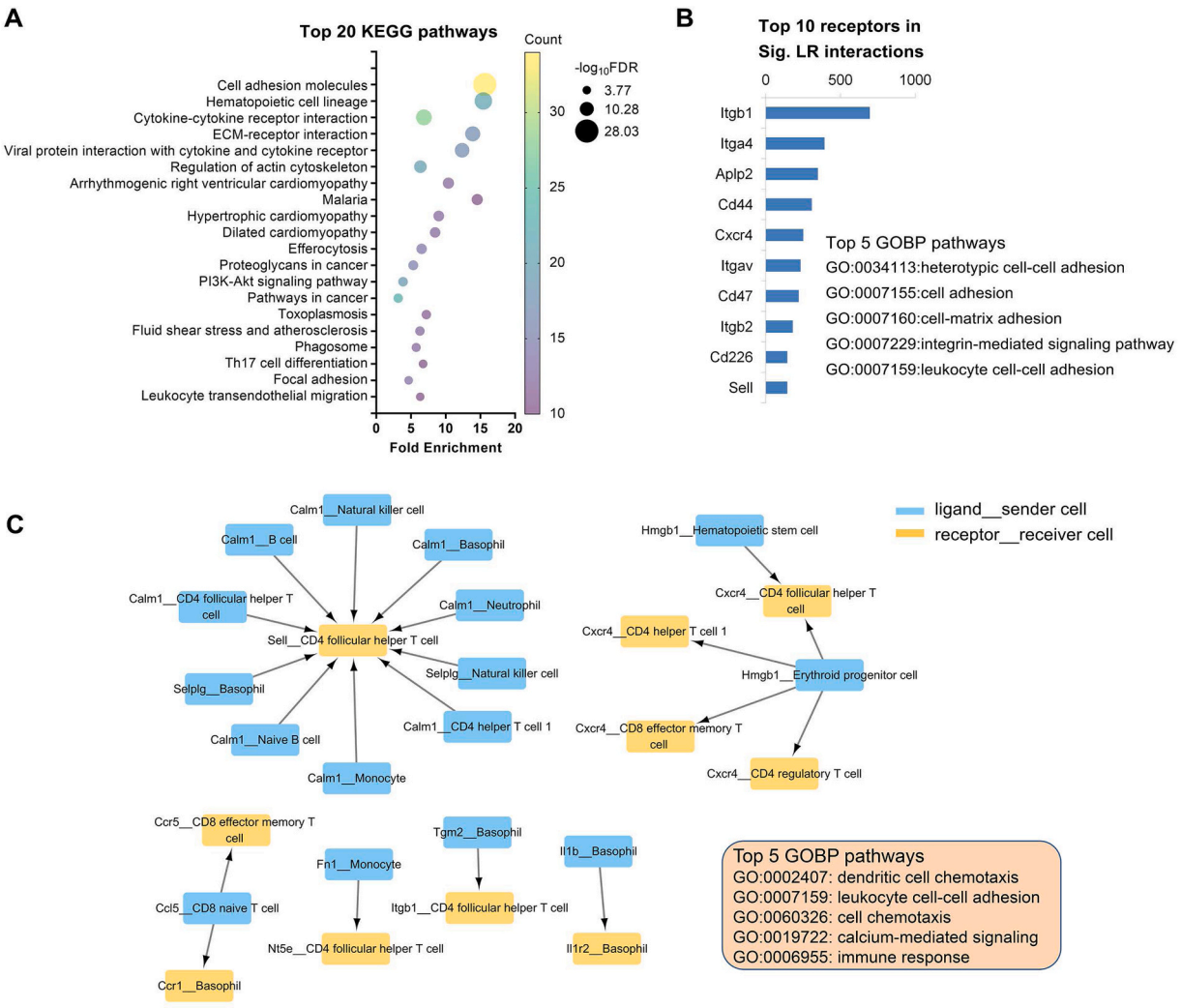

Fig. 3. Functional enrichment of differential LR interactions in old and young bone marrow. A. KEGG pathway enrichment of 144 receptors involved in 5560 significantly different LR interactions. Displaying the top 20 pathways (ordered by significance). B. Frequency statistics of receptors participating in significantly different LR interactions. The histogram shows the top 10 receptors. GOBP pathway enrichment was performed on these 10 receptors, and the top 5 pathways were displayed (ordered by significance). C. The cytoscape network diagram depicts the top 20 most significant differential LR interactions (10 up- and down-regulated in the old group). Blue represents the ligand and sender cell, and yellow represents the receptor and receiver cell. GOBP pathway enrichment was performed on the receptors, and the top 5 pathways with the highest significance were displayed.

[31]. The expression of ECM-receptor interaction-related genes changes significantly in fetal and elderly adult bone marrow mesenchymal stem cells [32].

Among the 144 receptor genes, the integrin family member Itgb1 is involved in the largest number of differential LR interactions as a receptor, with 697 interactions. Itgb1 serves as a key gene in ECM-integrin receptor interaction to regulate aging-related phenotypes [33]. The second largest number is another integrin gene Itga4, which is involved in 393 LR interactions. GO biological processes (GOBP) analysis of the top 10 receptor genes showed that the functions of these genes are mainly enriched in heterotypic cell-cell adhesion, cell adhesion and cell-matrix adhesion pathways (Fig. 3B).

The top 20 LR interactions with the largest differences between old and young (10 each with MS>0 and MS<0) are involved in 11 types of sender cells and 5 types of receiver cells. Among them, CD4 follicular helper T cell serves as the receiver cell most frequently. Follicular helper T cells (Tfh) are a T helper cell subset that play an important role in the differentiation of B cells into plasma cells [34]. In aging, the function of Tfh changes, resulting in a decrease in germinal center response, thereby reducing the immune response ability of the elderly [35]. These 20 differential LR interactions involve 7 receptor genes Il1r2, Ccr5, Ccr1, Cxcr4, Nt5e, Itgb1 and Sell. GOBP functional enrichment showed that these receptor genes were mainly enriched in dendritic cell chemotaxis, leukocyte cell-cell adhesion, and cell chemotaxis pathways (Fig. 3C).

2.4. Senescence-associated secretory phenotypes (SASPs) are involved in differential ligand-receptor interactions

SASP is a representative phenotype of cellular senescence and involved in cell-cell interactions [36]. Using the human homologous genes, we detected the distribution of SASP-related genes in different LR interactions. Among all 5560 differential LR interactions, 903 contained SASP-related genes, accounting for 16.2 % (Fig. 4A Left). A total of 20 SASP-related genes participated in these 903 significantly different LR interactions (Fig. 4B). Among them, Icam1 participates in 176 differential LR interactions, which is the most. Icam1 is intercellular adhesion molecule 1, which is usually expressed on the surface of endothelial cells and immune cells and is related to the occurrence of various diseases and organ aging [37–39]. This was followed by Tgfb1 and Mif, which participated in 159 and 157 differential LR interactions respectively.

In addition, 903 LR interactions including SASP-related genes involved 237 pairs of cells, accounting for 92.6 % of the total 256 cell

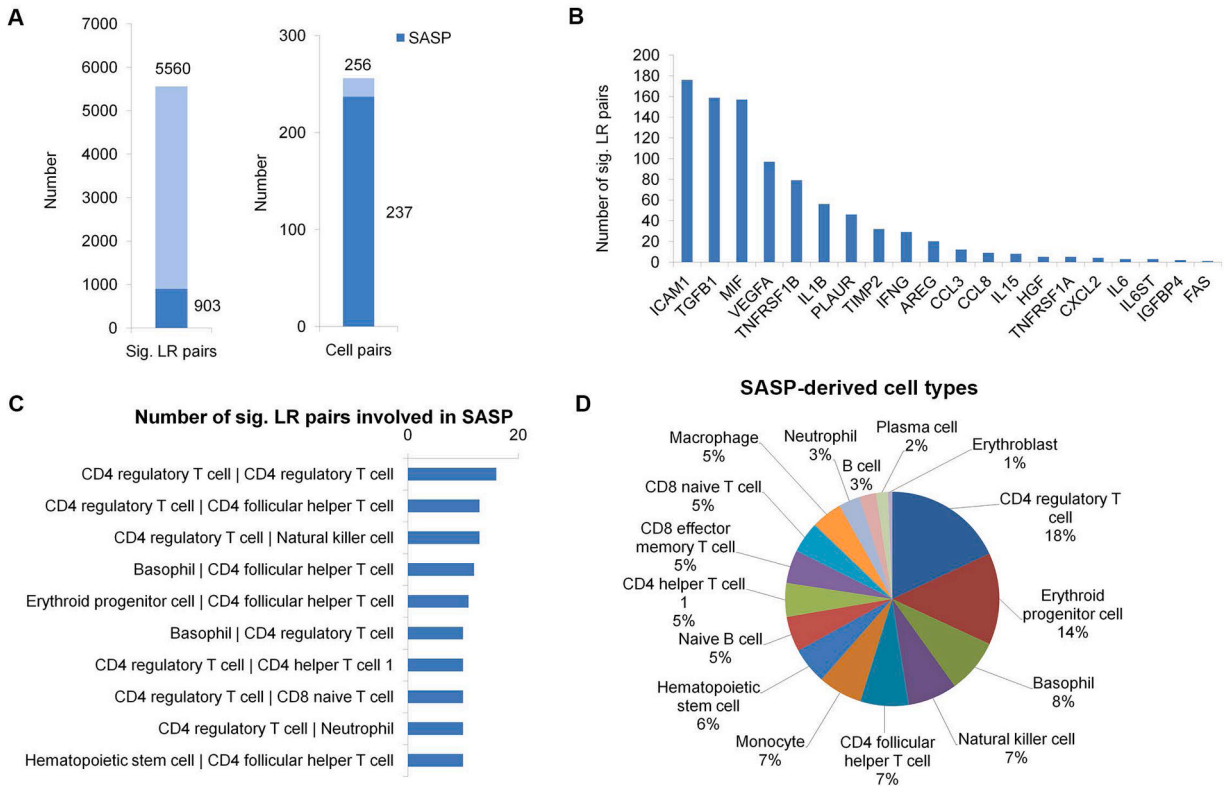

Fig. 4. SASP-related genes involves in differential LR interactions in old and young bone marrow. A. Left, among the 5560 significantly different LR interactions, 903 contain the SASP-related genes. Right, of the 256 pairs of cells with differential LR interactions, 237 pairs are involved in the SASP-related genes. B. Number of significantly different LR interactions involved in all 20 SASP-related genes. C. Top 10 cell pairs containing the significantly different LR interactions involved in SASP-related genes. D. Proportion of cell types involved in 903 LR interactions. SASP-related genes may act as ligands or receptors.

pairs, indicating that most cell-cell interactions involve SASP-related genes (Fig. 4A Right). Among them, we examined the cell pairs that contained the most LR interactions involving SASP-related genes, and found that the autocrine interaction of CD4 regulatory T cells contained 16 LR interactions involving SASP-related genes, which is the most. This is followed by the interaction between CD4 regulatory T cells and CD4 follicular helper T cells, and the interaction between CD4 regulatory T cells and natural killer cells, both containing 13 differential LR interactions involving SASP-related genes (Fig. 4C). This is consistent with previous reports that SASPs enhance and spread senescence in an autocrine and paracrine manner, and activates immune responses that eliminate senescent cells [40,41].

In the cell types containing in SASP-related genes (whether it is a sender cell or a receiver cell), CD4 regulatory T cell takes up the largest proportion (involving 163 interactions), followed by Erythroid progenitor cell (involving 125 interactions) (Fig. 4D). These results indicate that SASPs are deeply involved in cell-cell interactions in bone marrow aging.

2.5. *Senescent signs of HSCs are regulated by extracellular ligands*

As HSCs are the hematopoietic center of the bone marrow [42], we further examined whether aging affects ligand-receptor interactions between HSCs and other bone marrow cells. Among the 5560 significantly different LR interactions, a total of 598 interactions involved HSC. Among them, 301 interactions with HSCs serving as sender cells and 297 interactions with HSCs serving as receiver cells (Fig. 5A). Pathway enrichment of these receptors in 297 interactions are mainly enriched in cell adhesion, hematopoietic cell lineage, regulation of actin cytoskeleton and ECM-receptor interaction (Fig. 5B), which are related to HSC activities [43].

Among the 297 interactions with HSC serving as receiver cells, the LR score of 46 interactions decreased in the old group (MS < -0.1). We then considered whether increasing the interaction of these ligands and receptors could alter the senescent state of HSCs. Considering that ligands are easier to manipulate in vitro, we looked for those decreased ligand expression in aging bone marrow cells. In those 46 interactions, we observed the expression of three Ligands (Igfbp4, Mmp9, and Selenop) from CD8 naïve T cells decreased significantly and their corresponding receptors (Lrp6, Cd44, Itgb2 and Lrp8) in HSCs remained unchanged or increased in the elderly group. This indicates that the decrease in the expression of these ligands (Igfbp4, Mmp9, Selenop) may be the main factor leading to the decrease in LR scores in the old group.

As Igfbp4, Mmp9 and Selenop are all secreted proteins (UniProt database), we collected the supernatants of 293 T cells overexpressing these ligands to incubate HSCs extracted from the old mouse bone marrow. The supernatant of wild-type 293 T cells was used as a control. Flow cytometry analysis revealed that compared with the control supernatant, the percentage of β-Gal-positive HSCs treated with the three protein supernatants was significantly reduced (Fig. 5C). RT-qPCR experiment indicated the expression of aging-related genes p16 and p21 in HSCs were also decreased after ligand incubation (Fig. 5D). These results indicate that the addition of extracellular ligands have the potential to alter the senescent signs of hematopoietic stem cells, which provides new targets into the intervention of HSC senescence.

3. Discussion

By scoring the strength of ligand-receptor interactions, we detected a large number of differential ligand-receptor interactions between old and young bone marrow cells. These differential interactions arise from multiple cell types. For example, CD4 follicular helper T cell is the sender cell that participates in the most differential LR interactions and CD 8 naïve T, as a receptor cell, participates in the most differential LR

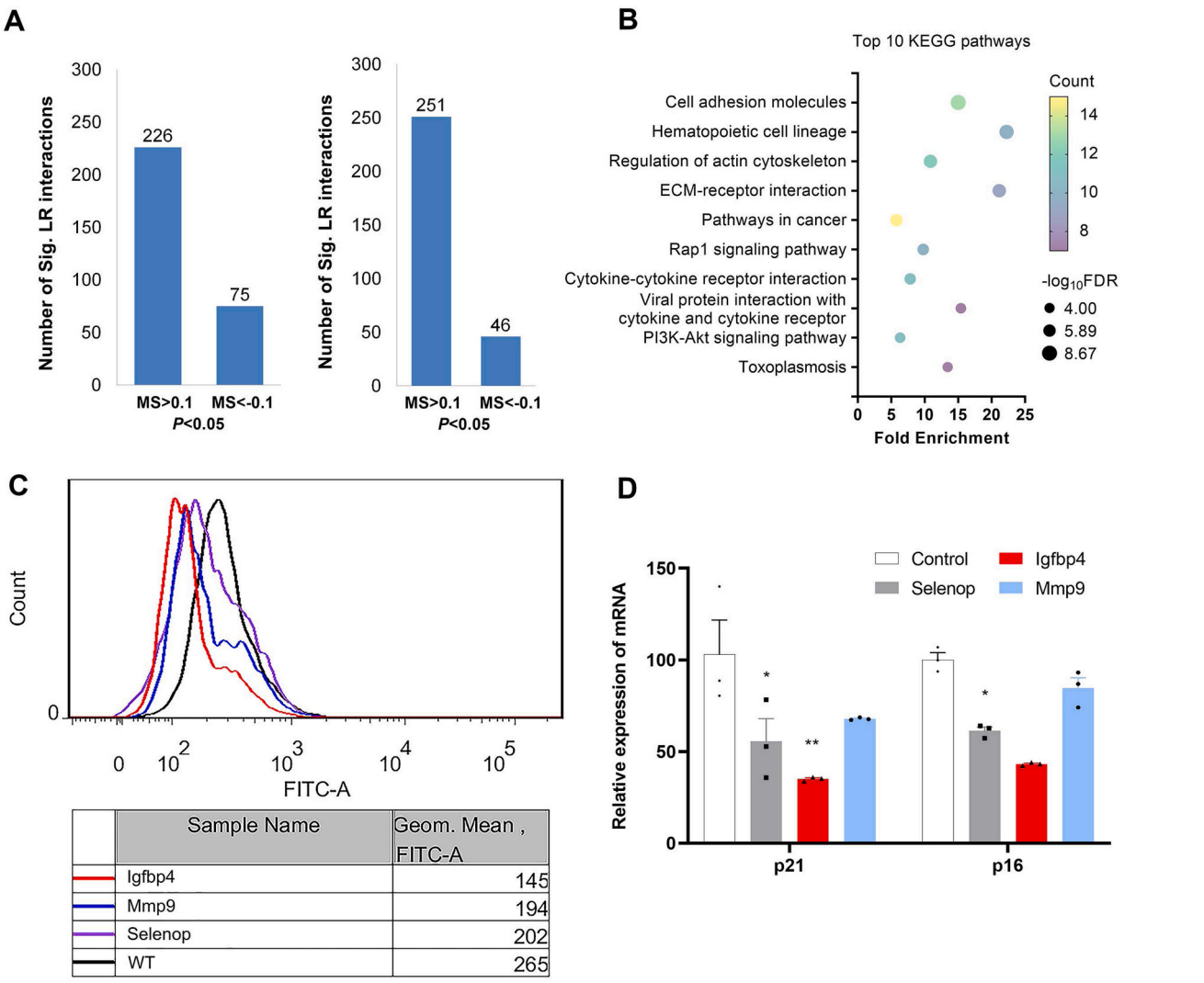

Fig. 5. Different LR interactions involving hematopoietic stem cells in old and young bone marrow. A. Left, the number of significantly different LR interactions with hematopoietic stem cells (HSC) as sender cell between the old and young group; Right, the number of significantly different LR interactions with HSC as receiver cell between the old and young group. MS> 0.1 and MS< −0.1 indicate up-regulation and down-regulation in the old group respectively. B . KEGG pathways enriched by receptors in the significantly different LR interactions with HSC as receiver cells. C, D. HEK293T cells were used to overexpress the three ligands Igfbp4, Mmp9 and Selenop respectively. Then the supernatant was then collected to incubate HSCs. WT is the supernatant of wild-type HEK293T without overexpressed protein. Then SPiDER-βGal flow cytometry was used to detect the fluorescence intensity of HSCs (C) and RT-qPCR was used to detect the expression of p16 and p21 in HSCs (D). * *P* value < 0.05, ** *P* value< 0.01.

interactions. Furthermore, some LR pairs appear frequently in differential interactions, such as Thbs1 and the integrin family members (Itgb1, Itgb2, Itga4), indicating their potential roles in bone marrow aging, which is consistent with previous reports [44,45]. The receptors in differential LR interactions are mostly involved in cell adhesion and hematopoietic cell lineage, which are related to bone marrow hematopoiesis and homeostasis [46,47]. These results confirm the significance of cellular communication in bone marrow aging.

In addition, SASP-related genes are frequently involved in the differential intercellular communication in aging. Our results indentified SASP-related genes such as Icam1, Tgfb1, etc. are involved in a number of differential LR interactions. These genes have been revealed to be involved in the emergence of cellular senescence phenotypes [39,48,49]. Furthermore, all 16 annotated cell types are involved in SASP-mediated LR interactions, further confirming that key roles of SASPs in bone marrow aging.

Interactions between HSCs and non-hematopoietic bone marrow cells are extensive and related to HSC states [8,43]. Our results confirm the extensive interactions between HSCs and non-adherent bone marrow cells and demonstrate that changes in extracellular ligands may influence HSC senescence. These ligands have been reported to be related to stem cell senescence, HSC regeneration, etc. [50–52]. However, since several non-hematopoietic cells such as mesenchymal stem cells (MSCs) were not identified in our dataset due to the sample preparation and sequencing resolution, the interactions between MSCs and HSCs are not inspected. This limitation can be addressed by performing specific cell sorting prior to single-cell library construction in the future work.

In summary, our work systematically identified and validated ligand-receptor interaction changes in the old and young bone marrow. These different interactions correspond to multiple cell types, exhibiting the extensive changes of intercellular communication in bone marrow aging. Our procedure can be used to discover potential markers of senescence and provide new clues for intervention in hematopoietic senescence.

4. Materials and methods

4.1. Sample collection

Bone marrow samples were acquired from six mice (C57BL/6 strain, three in 88 weeks and three in 6 weeks). All mice were housed and treated under the protocol approved by Animal Care and Use Committee of Huazhong Agricultural University. Mice were euthanized by cervical dislocation and femurs were removed. Non-adherent Bone marrow cells were flushed from the bone marrow cavities and brought into single-cell suspension by pipetting up and down. Cells were mixed with 3 ml of Mouse 1 × Lymphocyte Separation Medium (DAKEWE, 7211011) and covered on the surface of the cell suspension with 1 ml IMDM (Gibco, 12440053) medium. Residual red cells were lysed with red cell lysate (Solarbio life science R1010) on ice for 10 min, then washed twice (250 g for 10 min at 4 C) with ice-cold phosphate buffer saline (PBS).

4.2. 10x Genomics single-cell transcriptome sequencing

The protoplast suspension was loaded into Chromium microfluidic chips with 30 (v2or v3, depends on project) chemistry and barcoded with a 10X Chromium Controller (10X Genomics). RNA from the barcoded cells was subsequently reverse-transcribed and sequencing libraries constructed with reagents from a Chromium Single Cell 30v2 (v2 or v3, depends on project) reagent kit (10X Genomics) according to the manufacturer's instructions. Sequencing was performed with Illumina (NovaSeq 6000) according to the manufacturer's instructions (Illumina).

4.3. Single-cell transcriptome analysis

Single-cell sequencing reads were aligned to the mouse reference genome (mm10) using Cellranger (v7.1.0) with default parameters. Genes expressed in at least three cells were retained in the results. Cells with fewer than 200 genes and with mitochondrial gene expression greater than 5 % were excluded. Additionally, doublets were identified and removed using DoubletFinder [53]. The cleaned alignment results were then subjected to the standard Seurat [54] analysis pipeline for data dimensionality reduction and clustering of single-cell data. Each cluster was annotated based on marker information and differentially expressed genes identified by Seurat. Furthermore, integration of single-cell data from different samples was performed using Harmony [55]. All tools were run with default parameters.

4.4. Bone marrow cell annotation

Each cell type was annotated based on specific marker gene expression. The marker genes of 11 types of mouse bone marrow cells were obtained from CellTaxonomy [56], including: B cell, Basophil, Erythroblast, Erythroid progenitor cell, Hematopoietic stem cell, Macrophage, Plasma cell, Monocyte, Naive B cell, Natural killer cell, Neutrophil. In addition, in order to further subdivide T cell subpopulations, we obtained five T cell subtype marker genes from thermofisher (https://www.thermofisher.cn/): CD4 helper T cell 1, CD4 follicular helper T cell, CD4 regulatory T cell, CD8 effector memory T cell, CD8 naive T cell. All markers used for annotation are included in Table S2.

4.5. Pipeline to identify different ligand-receptor interactions

1) Use Seurat to obtain the gene expression (normalized counts) matrix and cell annotations of all cells in all samples.

2) Calculate the ligand and receptor expression of all cell pairs based on the normalized counts matrix, cell annotations, and published ligand-receptor database.

3) Calculate the interaction score of each pair of LR (LR score) according to the following formula: LR score = L_{exp}*R_{exp} / (L_{exp}+R_{exp}). L_{exp} and R_{exp} correspond to the ligand and receptor expression on the sender cell and receiver cell respectively.

4) The mean difference of LR scores in two groups (MS) is calculated and *P* value is determined by permutation test (1000 times).

4.6. LR database collection

The interactions of mouse ligand and receptor were collected from CellChat [16], CytoTalk [57], and celltalkDB [58]. A total of 3781 ligand-receptor pairs are included. Among them, 2575 LR pairs whose expression was observed in the annotated cells were retained.

4.7. Pathway analysis

Functional enrichment analysis was completed using DAVID (https://david.ncifcrf.gov/). Pathway information comes from KEGG (https://www.kegg.jp) [59] and GO (https://geneontology.org/) [60] databases. Human homologous SASP-related genes were extracted from previous work [36].

4.8. Flow cytometry

Bone marrow cells were collected with the same to 10x genomics single-cell sample preparation. The cells were blocked with anti-mouse CD16/32 (BD Biosciences, 553141), and divided equally into two parts. For the isolation of CD8 naïve T cells, cells were stained with APC-Cy7-conjugated CD3 (BD Biosciences, 557596), FITC-conjugated CD8 (BD Biosciences, 553030), APC-conjugated CD44 (BD Biosciences, 559250), PerCPCy5.5-conjugated CD62L (BD Biosciences, 560513) antibodies, and for the isolation of monocyte, cells were stained with PerCPCy5.5-conjugated CD11b (BD Biosciences, 561114), APC-conjugated Ly6C (BD Biosciences, 560595) antibodies. The fluorescence associated with live cells was measured with a FACS Calibur (BD Biosciences) and data were analyzed with FlowJo software.

4.9. RNA extraction and quantitative real-time PCR

Total RNA was isolated from cells using RNAiso plus (Takara, 108–95-2). A total of 0.5 μg RNA was reverse transcribed using PrimeScriptTM RT reagent kit (Takara, RR037A). The first-strand cDNA products were further diluted by seven-fold and used as PCR templates. RT-qPCR was performed on the BioRAD CFX96™ Touch (Bio-Rad Laboratories Inc.,) using SYBR Green Supermix (Vazyme, Q312–02). All samples were normalized with the expression level of Gapdh and primers used are listed in Table S3.

4.10. In vitro HSC cell senescence-associated β-galactosidase assays

Mouse Igfbp4 (Refseq ID: 16010), Mmp9 (Refseq ID: 17395), and Selenop (Refseq ID: 20363) were cloned into protein expression plasmids (Sino Biological Inc., Beijing, China). For polyethylenimine (PEI) transfection, each plasmid was transfected into HEK293T cells in two T-75 flasks. Untransfected wild-type HEK293T cells were used as control. The culture medium was harvested two days later and concentrated using a cutoff centrifugal filter unit (Millipore Sigma, Burlington, MA). Bone marrow cells were isolated from the leg bones of two 20-month-old female C57BL/6 mice, and then lymphocyte separation medium was used to isolate mononuclear cells. We then used a CD117 + sorting kit (Miltenyi Biotec, 130–097-146, CD117 MicroBeads) to select mouse CD117 + HSCs from mononuclear cells and seeded them into six-well plates. HSCs were cultured in BM medium containing CD3, CD6 and SCF to stimulate cell proliferation. Supernatants from HEK293T cells were added to incubate HSC cells in the next day. Cells were collected after 48 h and treated with a cellular senescence detection kit (SPiDER-βGal, Catalog number SG03) (Dojindo, Tokyo, Japan), followed by flow

cytometric analysis.

4.11. Statistical analysis

All statistical analyzes were performed using GraphPad Prism (GraphPad Software, La Jolla, CA) and R package (https://www.r-project.org/). Cytoscape (https://cytoscape.org/) is used to draw network diagrams.

Data and code availability

The raw sequence data reported in this paper have been deposited in the Genome Sequence Archive (https://ngdc.cncb.ac.cn/gsa/) (GSA: CRA012404, https://ngdc.cncb.ac.cn/gsa/s/l48JgxCz). The Perl code to implement the pipeline is available on github (https://github.com/GeneFeng/compareCCI).

Funding

This research was funded by National Natural Science Foundation of China (82170170) and the Fundamental Research Funds for the Central Universities (2662022SYYJ001).

CRediT authorship contribution statement

Lei Yao: Writing – original draft, Validation. **Jing Feng:** Software, Methodology. **Fengyue Li:** Writing – original draft, Validation. **Yuxin Shan:** Validation. **Shan Zhong:** Writing – review & editing, Supervision, Conceptualization. **Chunjiang He:** Writing – review & editing, Methodology, Conceptualization. **Wenbo Chen:** Writing – original draft, Formal analysis. **Xin Chen:** Writing – original draft, Validation. **Mingqian Feng:** Supervision, Conceptualization. **Linli Ren:** Validation. **Chenjian Zhuo:** Data curation.

Declaration of Generative AI and AI-assisted technologies in the writing process

No artificial intelligence (AI) and AI-assisted technologies were used in the writing process.

Declaration of Competing Interest

The authors declare no conflicts of interest.

Appendix A. Supporting information

Supplementary data associated with this article can be found in the online version at doi:10.1016/j.csbj.2024.06.020.

References

[1] Saheera S, Potnuri AG, Krishnamurthy P. Nano-Vesicle (Mis)Communication in Senescence-Related Pathologies. Cells 2020;9(9).
[2] Lopez-Otin C, et al. Hallmarks of aging: an expanding universe. Cell 2023;186(2):243–78.
[3] Bernet JD, et al. p38 MAPK signaling underlies a cell-autonomous loss of stem cell self-renewal in skeletal muscle of aged mice. Nat Med 2014;20(3):265–71.
[4] Kadota T, et al. Emerging role of extracellular vesicles as a senescence-associated secretory phenotype: Insights into the pathophysiology of lung diseases. Mol Asp Med 2018;60:92–103.
[5] Zhang G, et al. Hypothalamic programming of systemic ageing involving IKK-beta, NF-kappaB and GnRH. Nature 2013;497(7448):211–6.
[6] Ho YH, et al. Remodeling of bone marrow hematopoietic stem cell niches promotes myeloid cell expansion during premature or physiological aging. Cell Stem Cell 2019;25(3):407–18. e6.
[7] Young K, et al. Decline in IGF1 in the bone marrow microenvironment initiates hematopoietic stem cell aging. Cell Stem Cell 2021;28(8):1473–82. e7.
[8] Mende N, et al. Prospective isolation of nonhematopoietic cells of the niche and their differential molecular interactions with HSCs. Blood 2019;134(15):1214–26.
[9] Armingol E, et al. Deciphering cell-cell interactions and communication from gene expression. Nat Rev Genet 2021;22(2):71–88.
[10] Ennis S, et al. Cell-cell interactome of the hematopoietic niche and its changes in acute myeloid leukemia. iScience 2023;26(6):106943.
[11] Kokkaliaris KD, Scadden DT. Cell interactions in the bone marrow microenvironment affecting myeloid malignancies. Blood Adv 2020;4(15):3795–803.
[12] Cabello-Aguilar S, et al. SingleCellSignalR: inference of intercellular networks from single-cell transcriptomics. Nucleic Acids Res 2020;48(10):e55.
[13] Noel F, et al. Dissection of intercellular communication using the transcriptome-based framework ICELLNET. Nat Commun 2021;12(1):1089.
[14] Dries R, et al. Giotto: a toolbox for integrative analysis and visualization of spatial expression data. Genome Biol 2021;22(1):78.
[15] Garcia-Alonso L, et al. Mapping the temporal and spatial dynamics of the human endometrium in vivo and in vitro. Nat Genet 2021;53(12):1698–711.
[16] Jin S, et al. Inference and analysis of cell-cell communication using CellChat. Nat Commun 2021;12(1):1088.
[17] Pangrazzi L, Weinberger B. T cells, aging and senescence. Exp Gerontol 2020;134:110887.
[18] Lee NYS, et al. Establishing a human bone marrow single cell reference atlas to study ageing and diseases. Front Immunol 2023;14:1127879.
[19] Foulsham W, et al. Thrombospondin-1 in ocular surface health and disease. Ocul Surf 2019;17(3):374–83.
[20] Lu Y, et al. Identification of genetic signature associated with aging in pulmonary fibrosis. Front Med 2021;8:744239.
[21] Omatsu M, et al. THBS1-producing tumor-infiltrating monocyte-like cells contribute to immunosuppression and metastasis in colorectal cancer. Nat Commun 2023;14(1):5534.
[22] Wang F, et al. Aging-associated changes in CD47 arrangement and interaction with thrombospondin-1 on red blood cells visualized by super-resolution imaging. Aging Cell 2020;19(10):e13224.
[23] Olmos G, Lopez-Ongil S, Ruiz Torres MP. Integrin-linked kinase: a new actor in the ageing process? Exp Gerontol 2017;100:87–90.
[24] Wangler LM, et al. Amplified gliosis and interferon-associated inflammation in the aging brain following diffuse traumatic brain injury. J Neurosci 2022;42(48):9082–96.
[25] Ho TL, et al. HMGB1 promotes in vitro and in vivo skeletal muscle atrophy through an IL-18-dependent mechanism. Cells 2022;11(23).
[26] Peng Z, et al. PKR deficiency delays vascular aging via inhibiting GSDMD-mediated endothelial cell hyperactivation. iScience 2023;26(1):105909.
[27] Boczek T, et al. Cross talk among PMCA, calcineurin and NFAT transcription factors in control of calmodulin gene expression in differentiating PC12 cells. Biochim Biophys Acta Gene Regul Mech 2017;1860(4):502–15.
[28] Tanji-Matsuba K, et al. Functional changes in aging polymorphonuclear leukocytes. Circulation 1998;97(1):91–8.
[29] Lv J, et al. An aging-related immune landscape in the hematopoietic immune system. Immun Ageing 2024;21(1):3.
[30] Zhang Y, et al. CellCall: integrating paired ligand-receptor and transcription factor activities for cell-cell communication. Nucleic Acids Res 2021;49(15):8520–34.
[31] Erbaba B, et al. Zebrafish brain RNA sequencing reveals that cell adhesion molecules are critical in brain aging. Neurobiol Aging 2020;94:164–75.
[32] Liu X, et al. Analysis of hub genes involved in distinction between aged and fetal bone marrow mesenchymal stem cells by robust rank aggregation and multiple functional annotation methods. Front Genet 2020;11:573877.
[33] Liu X, et al. Withania somnifera root extract inhibits MGO-induced skin fibroblast cells dysfunction via ECM-integrin interaction. J Ethnopharmacol 2024;323:117699.
[34] Zhou M, et al. The effect of aging on the frequency, phenotype and cytokine production of human blood CD4 + CXCR5 + T follicular helper cells: comparison of aged and young subjects. Immun Ageing 2014;11:12.
[35] Linterman MA. How T follicular helper cells and the germinal centre response change with age. Immunol Cell Biol 2014;92(1):72–9.
[36] Gorgoulis V, et al. Cellular senescence: defining a path forward. Cell 2019;179(4):813–27.
[37] Chung YP, et al. Low-dose tributyltin triggers human chondrocyte senescence and mouse articular cartilage aging. Arch Toxicol 2023;97(2):547–59.
[38] Behnia F, et al. Chorioamniotic membrane senescence: a signal for parturition? Am J Obstet Gynecol 2015;213(3). p. 359 e1-16.
[39] Meyer K, et al. SARS-CoV-2 spike protein induces paracrine senescence and leukocyte adhesion in endothelial cells. J Virol 2021;95(17):e0079421.
[40] Acosta JC, et al. A complex secretory program orchestrated by the inflammasome controls paracrine senescence. Nat Cell Biol 2013;15(8):978–90.
[41] Serrano M, et al. Oncogenic ras provokes premature cell senescence associated with accumulation of p53 and p16INK4a. Cell 1997;88(5):593–602.
[42] Ng AP, Alexander WS. Haematopoietic stem cells: past, present and future. Cell Death Discov 2017;3:17002.
[43] Pinho S, Frenette PS. Haematopoietic stem cell activity and interactions with the niche. Nat Rev Mol Cell Biol 2019;20(5):303–20.
[44] Rohn F, et al. Impaired integrin alpha(5) /beta(1) -mediated hepatocyte growth factor release by stellate cells of the aged liver. Aging Cell 2020;19(4):e13131.
[45] Goddeeris MM, et al. Delayed behavioural aging and altered mortality in Drosophila beta integrin mutants. Aging Cell 2003;2(5):257–64.
[46] Dittel BN, et al. Regulation of human B-cell precursor adhesion to bone marrow stromal cells by cytokines that exert opposing effects on the expression of vascular cell adhesion molecule-1 (VCAM-1). Blood 1993;81(9):2272–82.

[47] Ambrosi TH, et al. Adipocyte accumulation in the bone marrow during obesity and aging impairs stem cell-based hematopoietic and bone regeneration. Cell Stem Cell 2017;20(6):771–84. e6.
[48] Marquez-Exposito L, et al. Acute kidney injury is aggravated in aged mice by the exacerbation of proinflammatory processes. Front Pharm 2021;12:662020.
[49] Fastova EA, et al. Analysis of bone tissue condition in patients with diffuse large B-cell lymphoma without bone marrow involvement. Bull Exp Biol Med 2020;169(5):677–82.
[50] Severino V, et al. Insulin-like growth factor binding proteins 4 and 7 released by senescent cells promote premature senescence in mesenchymal stem cells. Cell Death Dis 2013;4(11):e911.
[51] Lee MY, et al. Selenoproteins and the senescence-associated epitranscriptome. Exp Biol Med 2022;247(23):2090–102.
[52] Saw S, et al. Metalloproteases: on the watch in the hematopoietic niche. Trends Immunol 2019;40(11):1053–70.
[53] McGinnis CS, Murrow LM, Gartner ZJ. DoubletFinder: doublet detection in single-cell RNA sequencing data using artificial nearest neighbors. Cell Syst 2019;8(4):329–37. e4.
[54] Hao Y, et al. Integrated analysis of multimodal single-cell data. Cell 2021;184(13):3573–87. e29.
[55] Korsunsky I, et al. Fast, sensitive and accurate integration of single-cell data with Harmony. Nat Methods 2019;16(12):1289–96.
[56] Jiang S, et al. Cell Taxonomy: a curated repository of cell types with multifaceted characterization. Nucleic Acids Res 2023;51(D1):D853–60.
[57] Hu Y, et al. CytoTalk: De novo construction of signal transduction networks using single-cell transcriptomic data. Sci Adv 2021;7(16).
[58] Shao X, et al. CellTalkDB: a manually curated database of ligand-receptor interactions in humans and mice. Brief Bioinform 2021;22(4).
[59] Kanehisa M, et al. KEGG: integrating viruses and cellular organisms. Nucleic Acids Res 2021;49(D1):D545–51.
[60] Gene Ontology C, et al. The gene ontology knowledgebase in 2023. Genetics 2023;224(1).